Biomaterials 33 (2012) 4998–5003

Contents lists available at SciVerse ScienceDirect

Biomaterials

journal homepage: www.elsevier.com/locate/biomaterials

Nanotopography as modulator of human mesenchymal stem cell function

Karina Kulangara, Yong Yang, Jennifer Yang, Kam W. Leong*

Department of Biomedical Engineering, 136 Hudson Hall, Box 90281, Duke University, Durham, NC 27708, USA

ARTICLE INFO

Article history:
Received 31 December 2011
Accepted 15 March 2012
Available online 18 April 2012

Keywords:
Cell adhesion
Image analysis
Nanotopography
Mesenchymal stem cells

ABSTRACT

Nanotopography changes human mesenchymal stem cells (hMSC) from their shape to their differentiation potential; however little is known about the underlying molecular mechanisms. Here we study the culture of hMSC on polydimethylsiloxane substrates with 350 nm grating topography and investigate the focal adhesion composition and dynamics using biochemical and imaging techniques. Our results show that zyxin protein plays a key role in the hMSC response to nanotopography. Zyxin expression is downregulated on 350 nm gratings, leading to smaller and more dynamic focal adhesion. Since the association of zyxin with focal adhesions is force-dependent, smaller zyxin-positive adhesion as well as its higher turnover rate suggests that the traction force in focal adhesion on 350 nm topography is decreased. These changes lead to faster and more directional migration on 350 nm gratings. These findings demonstrate that nanotopography decreases the mechanical forces acting on focal adhesions in hMSC and suggest that force-dependent changes in zyxin protein expression and kinetics underlie the focal adhesion remodeling in response to 350 nm grating topography, resulting in modulation of hMSC function.

1. Introduction

Tissue regeneration and cell-based therapies often require a supporting scaffold to optimize cell function. Interestingly substrate nanotopography has been shown to influence the differentiation or maintain the stemness of human mesenchymal stem cells (hMSC) depending on the topographical features [1–3]. Recent literature presents many interesting findings on how nanotopography facilitates cell adhesion, alters cell morphology, affects proliferation, initiates intracellular signaling, provides contact guidance and mediates stem cell differentiation [4]. However little is known about the molecular mechanisms underlying the cellular response to substrate topography. Namely, how is nanotopography sensed by the cell, what molecules are necessary in this process, and most importantly how does this influence the cellular functions? Understanding the molecular mechanism is crucial to the better design of a scaffold for a given application or to combine substrates with biochemical cues to enhance the modulatory effect of cell–topography interactions.

Human mesenchymal stem cells (hMSCs) are marrow-derived, self-renewing cells with multipotent differentiation potential. They give rise to various anchorage-dependent cell types, including adipocytes, chondrocytes, myoblasts, and osteoblasts [5]. Their differentiation potential is influenced by substrate elasticity [6], geometrical confinement [7],[8], and substrate topography [1–3].

Cell-substrate or cell-extracellular matrix (ECM) adhesions are mediated by dynamic multiprotein structures called focal adhesions (FA). They are important for force transmission, cytoskeletal regulation and signaling. At these sites the cell establishes a transmembrane connection between elements of the ECM and the actin cytoskeleton [9]. The transmembrane integrin proteins orchestrate these events [10]. The integrins, heterodimers containing one α- and one β– subunit, bind with their extracellular domain to the ECM proteins fibronectin, laminin, and vitronectin.

The cytosolic domain of integrins binds to a large number of proteins such as paxillin and zyxin either directly or via scaffolding proteins [11]. Some of these proteins are implicated in strengthening the linkage between the extracellular matrix and the cytoskeleton, others play a role in adhesion-mediated signaling [12]. Cellular adhesions can be classified into three categories: Focal complexes (FX), FA and fibrillar adhesions [13]. The FX along the leading lamella of migrating cells are early adhesions, which transform into focal adhesion upon RhoA activation [14,15] or as a result of external mechanical perturbation [16,17]. Fibrillar adhesions develop from FAs following actomyosin contraction [18,19]. Recruitment of zyxin protein has been proposed as a molecular marker for mature FAs [20]. Zyxin facilitates actin polymerization in response to mechanical forces [21] and dissociates from focal adhesions upon force dissipation [22].

* Corresponding author. Tel.: +1 919 660 8466; fax: +1 919 684 6608.
E-mail address: kam.leong@duke.edu (K.W. Leong).

0142-9612/$ – see front matter © 2012 Elsevier Ltd. All rights reserved.
doi:10.1016/j.biomaterials.2012.03.053

Focal adhesions are closely linked to cellular migration, which is driven by repeated cycles of protrusion of the leading edge, formation of new matrix adhesions and retraction of the trailing edge. FA play a dual role in motility. On one hand they provide a robust anchor to the ECM, necessary for the actomyosin system to exert the force to pull the cell body and the trailing edge forward, but on the other hand they may also restrain the migration process [23,24]. On planar substrates cellular movement is traditionally characterized as a persistent random walk. In this conceptual model, cells migrate along a fairly straight path during short time intervals, whereas over longer time intervals, the cells execute random changes in a directional manner.

To investigate the underlying mechanisms of nanotopography-modulated hMSC behavior we performed studies on poly-dimethylsiloxane (PDMS) substrates with planar or 350 nm grating topography. We used western blotting, immunocytochemistry and confocal microscopy to identify changes in focal adhesion composition on 350 nm topography compared to planar control. We used fluorescence recovery after photobleaching (FRAP) in live cell microscopy to relate FA dynamics with differences in migration behavior.

2. Materials and methods

2.1. Fabrication of PDMS nanogratings substrates

Nanogratings of 350 nm linewidth, 700 nm pitch, and 280 nm depth were written in a poly(methylmethacrylate) (PMMA) thin film that was spin-coated onto a Si substrate using electron beam lithography (EBL) as previously described [25,26]. Substrates with no features or 350 nm topography for cell culture were replicated in PDMS because of the ease of fabrication. A mixture of PDMS resin and curing agent (SYLGARD 184 kit, Dow Corning, MI, USA) in a 10:1.05 w/w ratio was poured onto the EBL mold and degassed in a vacuum chamber for 60 min. After curing for 2 h at 65 °C, and once the PDMS reached RT the inverse PDMS mold was peeled from the EBL mold. The PDMS mold with nanogratings was utilized for cell culture. PDMS substrates were sterilized by ethanol, followed by UV exposure for 30 min. For cell culture the PDMS substrates were coated with collagen I (BD Biosciences, Bedford, MA) at 15 μg/cm^2 to enable hMSC attachment [27].

2.2. Scanning Electronic Microscopy (SEM)

The nanogratings and microchannels were sputter-coated with a gold layer ~10 nm thick using a Denton Vacuum Desk IV sputter unit at 75 mTor and 18 mA (Denton Vacuum, LLC, Moorestown, NJ, USA). SEM micrographs were obtained from a FEI XL30 SEM-FEG (FEI Co., Hillsboro, OR, USA).

2.3. Cell culture and antibodies

Human MSCs were supplied by Dr. D. Prockop from Tulane Center for Gene Therapy at Tulane University, New Orleans, LA, USA [28]. The hMSCs used in the experiments were at passages 3–6. hMSCs were cultured in complete culture media (CCM) comprising α-Minimum Essential Medium (α-MEM) supplemented with 16.5% (v/v) fetal bovine serum (FBS, Atlanta Biologicals, Inc., Lawrenceville, GA, USA), 2 mM L-glutamine (Gibco/Invitrogen, Carlsbad, CA, USA), 100 U/ml penicillin, and 100 mg/ml streptomycin (Gibco/Invitrogen, Carlsbad, CA, USA). The cells were seeded at a density of 3000 cells/cm^2 and placed in an incubator under 5% CO_2 [29,30].

Antibodies against the following proteins were applied for Western blotting (W) or immunofluorescence (IF). Monoclonal antibodies: zyxin 1:500 (W), 1:200 (IF) (Abcam, Cambridge, MA, USA), GAPDH 1:5000 (W) (Abcam, Cambridge, MA, USA), Integrin β3 1:500 (W) (BD, Franklin Lakes, NJ, USA), Integrin β1 1:1000 (W), (Millipore, Billerica, MA, USA), paxillin 1:1000 (W), 1:200 (IF) (Epitomics, Burlingame, CA, USA). Secondary antibodies used for IF were Alexa Fluor 594 goat anti-rabbit secondary antibody (1:200; Invitrogen, Carlsbad, CA, USA), or Alexa Fluor 488 goat anti-mouse secondary antibody (1:200; Invitrogen, Carlsbad, CA, USA), secondary antibodies used for Western blot were HRP-conjugated goat anti-mouse antibody (1:5000; Novagen, Merck, Darmstadt, Germany) and HRP-conjugated goat-anti-rabbit antibody (1:3000; Biorad, Hercules, CA, USA). F-actin was stained with Alexa Fluor 488 phalloidin (Invitrogen, Carlsbad, CA, USA), and the cell nuclei were stained with 4,6-Diamidino-2-phenylindole (DAPI, Molecular Probes, Invitrogen, Carlsbad, CA, USA).

2.4. Western blotting

For analysis of focal adhesion composition, whole cell lysates were collected. Cells were washed in PBS containing Mg^{2+} and Ca^{2+} and lysed in cold lysis buffer (20 mM HEPES/KOH pH 7.4, 2 mM EDTA, 2 mM EGTA, 0.1 mM DTT) containing 0.1 M KCl, 0.3 mM PMSF, 0.7 μg/ml Pepstatin, 2 μg/ml Aprotinin, 2 μg/ml Leupeptin. For Western blotting proteins were diluted in 2X Laemmli buffer (Sigma-Aldrich, Germany), separated on SDS-PAGE and transferred onto PVDF or nitrocellulose membrane (Biorad, Hercules, CA, USA), blocked with 5% non-fat milk in TBS containing 0.01% Tween-20 (Sigma-Aldrich, Germany) for 1 h at room temperature and probed with the indicated antibodies overnight at 4 °C, after 3 washes in TBS containing 0.01% Tween-20, the membranes were incubated for 1 h at room temperature with the indicated secondary antibodies. Antibody bands were then detected and quantified using the ECL Plus detection kit according to the manufacturer's recommendations (GE Healthcare, USA) on a Fluorchem FC2 imaging system detecting chemiluminescence (Alpha-Innotech, CA, USA).

2.5. Immunofluorescence staining

Human MSCs were fixed with 4% parafomaldehyde in PBS for 15 min at room temperature, permeabilized with 0.3% Triton X-100 (Sigma-Aldrich Co.) and stained in a blocking solution containing the mentioned antibodies. The blocking solution consisted of 0.03 g/ml bovine serum albumin (BSA, Sigma-Aldrich Co.) and 10% goat serum (Sigma-Aldrich Co.) in 0.3% Triton X-100 (Sigma-Aldrich Co.) in PBS for 2 h. The samples were washed 3x before incubation with the secondary antibody in blocking solution for 1 h at RT. The samples were then mounted in Fluoro-Gel (Electron Microscopy Sciences, Hatfield, PA, USA) for fluorescent imaging and viewed with Zeiss LSM 510 inverted confocal microscope using a 63× objective with a NA of 1.4.

2.6. Confocal, time-lapse microscopy and image analysis

The time-lapse DIC images (4× objective) were collected with a cooled CCD camera (CoolSnap HQ; Photometrics, Tucson, AZ, USA) at 2.5 min intervals by using a Zeiss Axiovert microscope. The microscope was equipped with an incubation chamber, which controlled the temperature, humidity and 5% CO2. The images were processed using *Metamorph* software, approximately 20 cells were analyzed for each condition. Briefly, cells were tracked using the metamorph tracking function for objects and the resulting tracks tested for directionality compared to the grating direction.

Images for quantification of focal adhesion size were aquired using a Zeiss LSM 510 inverted confocal microscope. 15 images from each of three replicates were collected for each condition. Approximately 1000 focal adhesions for each condition were analyzed using *Imaris* software. Briefly, after setting a threshold; particles of sizes between 2 and 10 μm^2, the typical size range for mature focal adhesions [13] were extracted and analyzed. Student's *t*-test was used to compare the average focal adhesion size between conditions.

2.7. Lentiviral production

Zyxin-GFP was obtained from Dr. Rottner and Dr. Petroll and was subcloned into the FUGW lentiviral vector (Addgene, Cambridge, MA, USA). Zyxin-GFP was cut from pEGFP vector using first NotI followed by blunting using the DNA Polymerase I, Large (Klenow) Fragment (New England Biolabs, Ipswich, MA, USA) and subsequent digestion with BglII, FUGW was linearized using EcoR1 followed by blunting and subsequent digestion with BamH1. After the removal of 5′ phosphate groups from FUGW using the Antarctic Phosphatase (New England Biolabs, Ipswich, MA, USA), the constructs were ligated using the Rapid ligation kit (Roche, Basel, Switzeland) according the manufacturer's protocol. Stabl3 bacteria (Invitrogen, Carlsbad, CA, USA) were transformed according to the manufacturer's protocol. Plasmid DNA was purified using the Maxiprep kit from Qiagen (Germantown, MD, USA) according to the manufacturer's protocol. For the lentiviral production 75 cm^2 dishes with 293T cells, cultured in DMEM (Gibco, Invitrogen, Carlsbad, CA) containing 10% fetal bovine serum (Altanta Biologicals, Lawrenceville, GA) and 1% penicillin-streptomycin (Gibco, Invitrogen, Carlsbad, CA) were transfected by the calcium phosphate technique with the following plasmids: 16.9 μg of pMD2.G (Addgene plasmid 12259) 31.3 μg of psPAX2 (Addgene plasmid 12260) and 48.2 μg of GFP-zyxin in the FUGW vector (Addgene plasmid 14883) [31]. The medium was changed after 14 h. 72 h after transfection the medium was collected in 50 ml tubes and spun to remove cell debris. The supernatant is concentrated to 100x in Amicon Ultra centrifugal filter tubes, (Millipore,Tullagreen, Irland) and the concentrated virus kept at −80 °C. HMSC were infected with 5 μl of 100x viral concentrate in cell culture medium.

2.8. Fluorescence recovery after photobleaching (FRAP)

FRAP experiments were performed on the Leica DMI6000CS confocal microscope using a 63x/1.20 water objective. The 488 nm line of an Argon/2 multiple-lined single-photon laser source (5% of full power) was used for GFP excitation; 100% of the 488 nm line was used for photobleaching with 3 iterations corresponding to

1.25 s. The recovery curves were obtained using the FRAP wizard in the Leica software and measured recovery curves were normalized to the amount of photobleached protein, and fitted to a single exponential. To test equality of means for the $\tau_{1/2}$ values measured under different conditions, statistical analyses were performed using the Student's *t*-test (*graphpad*). The sample size for all *t*-tests was more than 40.

3. Results

3.1. hMSC migration on planar versus 350 nm topography

We observed here as previously described [27] that hMSC aligned in the 350 nm grating direction compared to the planar control substrates (Fig. 1). This observation prompted us to investigate in more detail the migration behavior of hMSCs on these 350 nm gratings. 36 h live cell imaging and tracking of the hMSC's trajectories revealed that the cells adopted a random walk motility on the planar surfaces, whereas on the 350 nm gratings the hMSCs migrated along the grating direction. Cell–cell contact overruled the directionality in migration on the grating substrates. Interestingly hMSC migrated at a speed of 15.6 μm/h on 350 nm gratings, significantly higher than the 8.3 μm/h observed on planar controls (Fig. 2 and supplementary movies 1 and 2 on planar and 350 nm substrates, respectively).

Supplementary video related to this article can be found at doi: 10.1016/j.biomaterials.2012.03.053.

3.2. Focal adhesions on planar versus 350 nm topography

We hypothesized that 350 nm gratings would alter the adhesion structures of hMSCs compared to planar substrates. In a previous study we characterized the nuclear alignment of hMSC to 350 nm topography in a 48 h time-course after cell seeding [32]. In this study we showed that the cell's alignment to substrate topography began at 8 h and continued for 48 h. To ensure observation of a clear effect of substrate topography on FAs we chose to analyze the focal adhesion composition at 36 h after cell seeding. HMSC lysates on planar versus 350 nm gratings were tested by Western blot. We tested for integrin β1, integrin β3, two transmembrane proteins characteristic for FA and focal contacts, and the two scaffold proteins paxillin and zyxin. Interestingly we did not observe any significant difference in protein level for integrin β1, integrin β3 and paxillin normalized to GAPDH. Zyxin protein expression however, was significantly decreased in hMSCs cultured on 350 nm gratings (Fig. 3A). Densitometry of the bands normalized to GAPDH revealed a 40% decrease in zyxin protein expression (Fig. 3B).

We then proceeded to test by immunocytochemistry if the size or number of mature focal adhesion structures was different. We analyzed confocal images for zyxin staining on planar versus 350 nm gratings (4A, C) using *Imaris*, and compared structures between 2 and 10 μm^2 (4B, D), the typical size for mature focal adhesions [13]. On 350 nm gratings we observed a significant reduction of average mature FA size by about 40% to 3.2 ± 0.26 μm^2 compared to 5.3 ± 0.55 μm^2 on planar controls (Fig. 4E). The number of mature FA structures detected was not significantly different between 350 nm and the planar substrates (data not shown). Note that the mature FA followed the grating direction and oriented the cells along the grating axis.

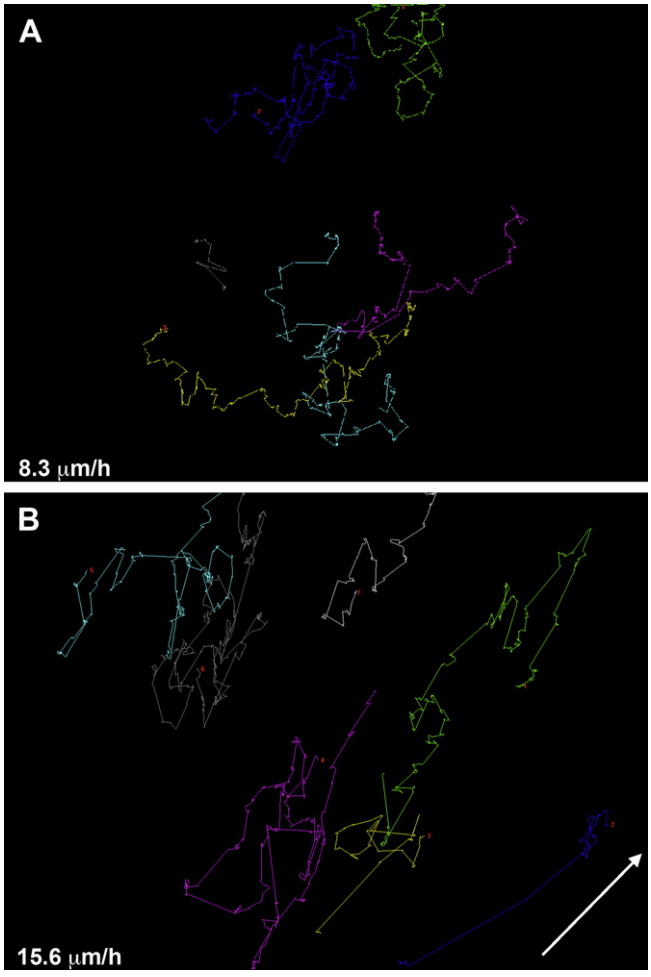

Fig. 2. (A) Migration of hMSC on planar substrates is a random walk. (B) On 350 nm gratings hMSC predominantly migrate along the grating direction with increased migration speed. The arrow illustrates the grating direction.

3.3. Zyxin turnover in FA on planar versus 350 nm topography

We explored the FA dynamics of hMSCs cultured on 350 nm gratings versus planar controls and tested whether there was

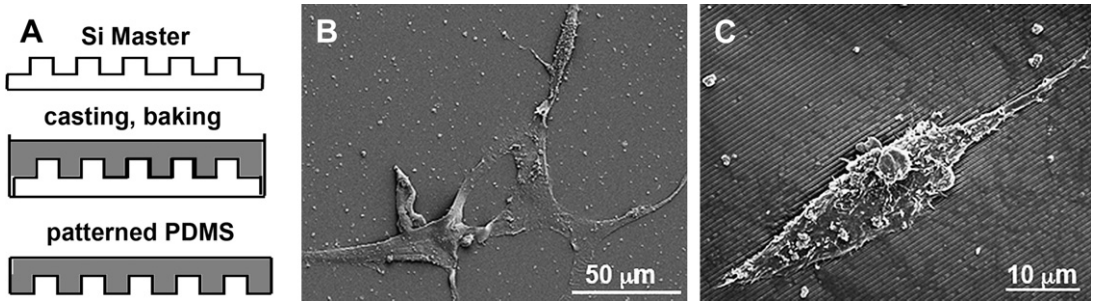

Fig. 1. HMSC sense and orient along 350 nm grating topography. (A) Schematic illustration of the fabrication of nanogratings on PDMS. SEM images of hMSC on planar PDMS (B) and 350 nm grating substrates (C).

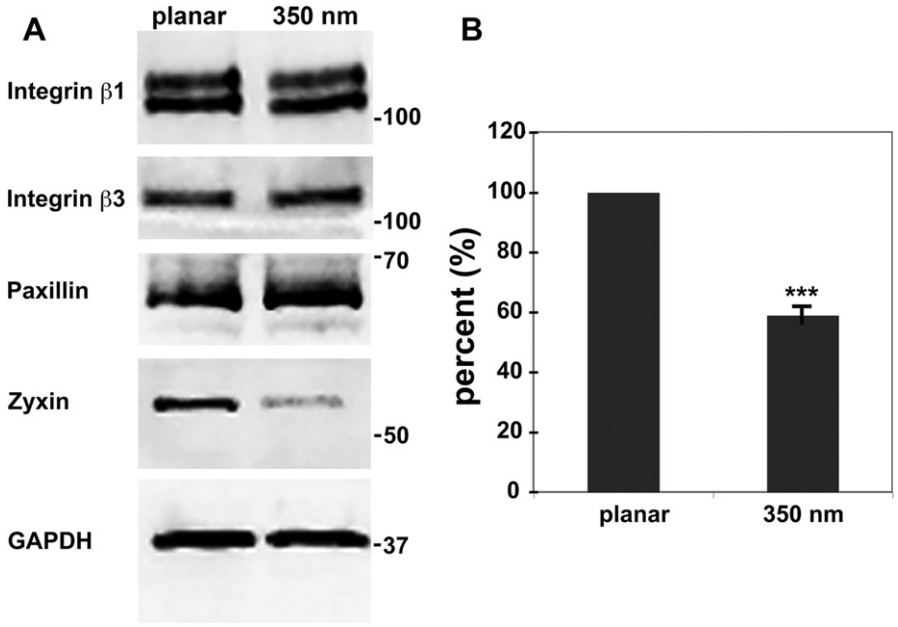

Fig. 3. Western blot analysis of focal adhesion proteins on planar and 350 nm nanogratings. (A) HMSCs show no significant change in transmembrane focal adhesion proteins integrin β1 and β3, and the scaffold protein paxillin. The protein zyxin however, found in mature focal adhesion was markedly decreased in hMSCs on 350 nm gratings. (B) Quantification of bands using densitometry, normalized for GAPDH and shown as percentage of planar controls.

a difference in zyxin dissociation from FA in hMSC on 350 nm gratings compared to planar controls. An elegant way to assess the FA dynamics is using FRAP (fluorescence recovery after photobleaching). We infected hMSC with lentiviral vectors containing a GFP-zyxin fusion protein [33] and photobleached GFP-zyxin in an area of 1 μm diameter within a focal adhesion to minimize the photobleaching of freely diffusing cytoplasmic GFP-zyxin protein. In this case the recovery curve reflects the binding and unbinding kinetics of GFP-zyxin within the FA [22]. Normalized fluorescence recovery curves for GFP-zyxin in hMSC on planar substrates (squares) and in hMSC on 350 nm substrates (triangles) are shown in Fig. 5B. In hMSCs cultured on 350 nm gratings we observed a $\tau_{1/2}$ recovery of fluorescence of 5.3 s, compared to 9.2 s for hMSCs on planar control substrates (Fig. 5C). This indicates that the turnover

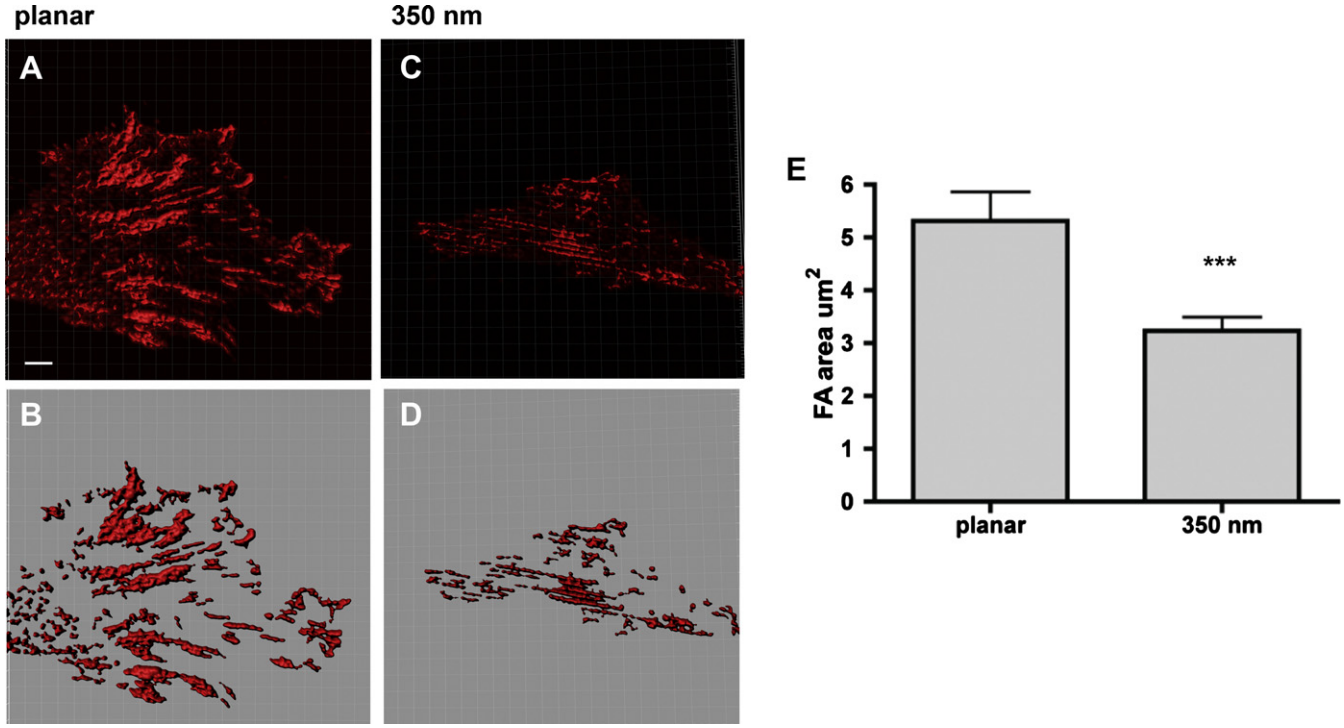

Fig. 4. Mature focal adhesions are smaller on 350 nm gratings compared to planar controls. HMSCs on planar (4A) and 350 nm gratings were stained for zyxin protein (4C) and zyxin-positive adhesions were extracted after applying a threshold (4B,D). Mature FA were quantified on planar versus 350 nm grating substrates (4E).

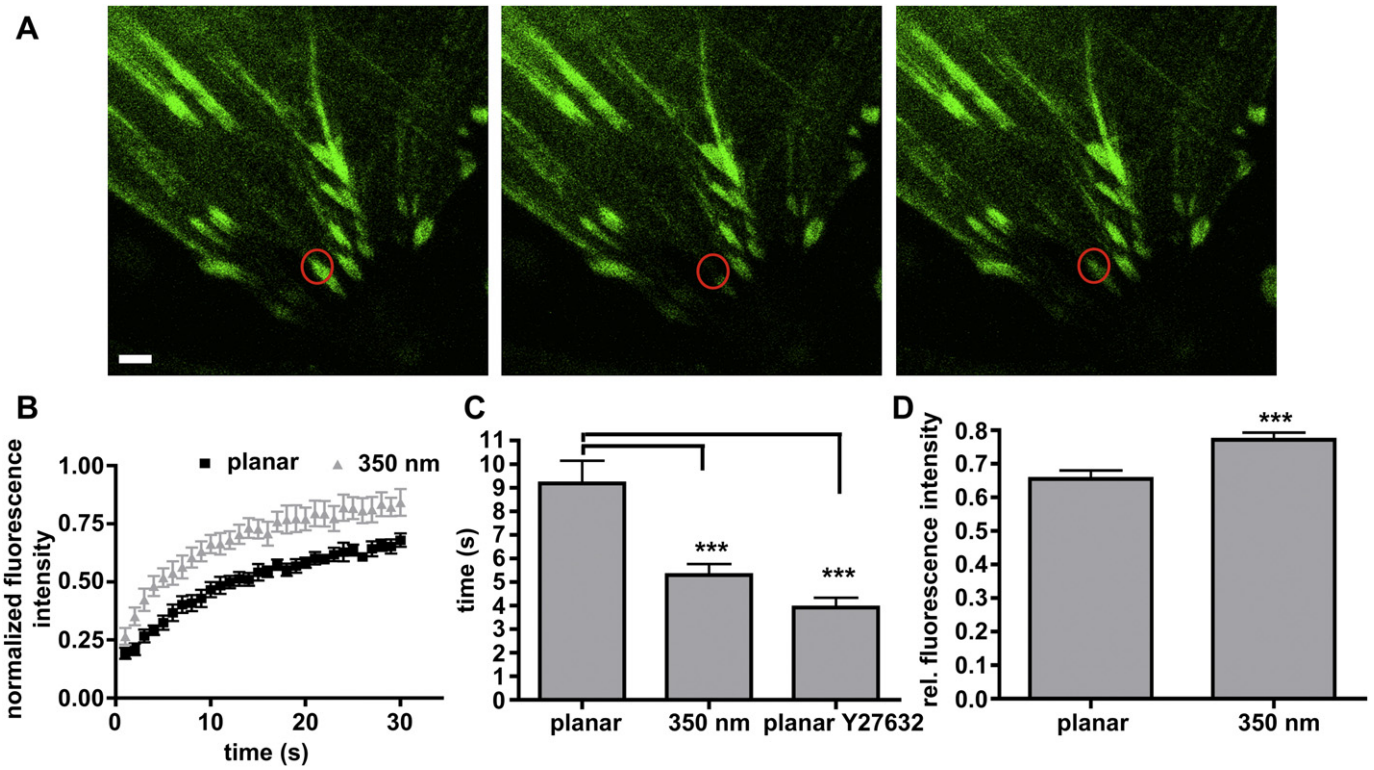

Fig. 5. Mature FA dynamics is altered on 350 nm gratings. FRAP was used to bleach a portion of GFP-zyxin assembled in FA (5A). Scale bar 2 μm. Fluorescence recovery curves of GFP-zyxin on planar and 350 nm gratings (5B). The $\tau_{1/2}$ of GFP-zyxin on 350 nm gratings was significantly faster compared to $\tau_{1/2}$ of GFP-zyxin on planar substrates and similar to $\tau_{1/2}$ of GFP-zyxin in hMSC treated with the Rho kinase inhibitor Y27632 (5C). A higher mobile fraction of GFP-zyxin protein also indicates a more dynamic exchange of zyxin protein in FA on 350 nm nanogratings compared to planar controls (5D).

of GFP-zyxin proteins is increased on 350 nm gratings. In addition we observed a higher mobile fraction of GFP-zyxin in hMSC on 350 nm topography compared to planar control substrates, also indicating a higher turnover rate of GFP-zyxin on 350 nm topography substrates (Fig. 5D). Interestingly we observed a similar increase in turnover rate with a $\tau_{1/2}$ of 3.9 s when we treated hMSCs on planar substrate with the Rho-associated kinase (ROCK) inhibitor Y27632 (Fig. 5C). The ROCK inhibitor dissipates cytoskeletal tension without disrupting microfilament integrity. Such an increase upon ROCK inhibitor treatment in $\tau_{1/2}$ for GFP-zyxin has been previously observed in endothelial cells on tissue culture polystyrene [22].

4. Discussion

Zyxin is recruited to focal adhesions upon their maturation [13] and it has emerged as a key player in mechanotransduction at cell adhesive structures [34]. Our results demonstrate that zyxin protein is a key player in nanotopography-mediated changes in hMSC function. We showed by Western blot that total zyxin protein is downregulated in hMSCs cultured on 350 nm gratings, which relates to the smaller mature FA sizes observed by immunocytochemistry in hMSCs on 350 nm topography compared to planar control substrates. We have previously shown that substrate topography influences FA composition [27] and zyxin has been identified in a 2 DiGE screen to play a role in topography sensing of osteoprogenitor cells [35]. Interestingly the topography employed in the paper by Kantawong et al. is a pitted array, indicating the zyxin protein is important in orchestrating the cellular response to a variety of nanoscale topographies and not only gratings. The smaller size of mature FA also explains the observation that hMSC migrate faster on PDMS substrates with 350 nm grating topography. FAs anchor hMSCs to the substratum; in this context smaller FAs represent a laxer anchorage that is less restrictive to the migration process [36]. HMSC are primarily guided in the grating direction. Cell–cell interaction however overruled the cell–topography interaction and may steer the hMSC away from their directional path. FA are multifunctional structures that mediate not only cell-ECM adhesion but also force transmission, cytoskeletal regulation and adhesion-dependent signaling. In the context of mesenchymal stem cells, anchorage to the stem cell niche is necessary for their self-renewal capacity and migration out of the niche is necessary for their differentiation.

Zyxin is not only a hallmark of mature FA but also a crucial player in force sensing and force transmission. Zyxin dissociates from FA upon dissipation of force [22]. Our results show a higher turnover rate of zyxin-GFP protein expressed in hMSCs on 350 nm gratings compared to planar control substrates. The $\tau_{1/2}$ of 9.2 s on planar PDMS substrates are in nice agreement with previous reports that showed that the exchange of individual proteins between FA and the cytoplasmic pool occurs over a period of seconds, whereas the adhesion disassembly occurs over a period of minutes [22,37]. Mechanical forces are known to influence the structure of FAs: Cellular contractility is necessary for the development of FA [38], and under force the FAs grow larger [39]. In turn the stability of the linkage between the integrins and the actin cytoskeleton is necessary for maintaining a FA; the dissection of this linkage leads to the disassembly of FAs [40]. Zyxin dissociates from FA when the mechanical load is reduced by inhibiting the actomyosin interaction, ablating individual stress fibers, or softening the substratum [22,33,41]. Smaller adhesion size holds reduced mechanical load [39], and especially smaller zyxin-positive structures suggest less force acting on these FAs. Our results measuring an accelerated zyxin turnover rate by FRAP on 350 nm

gratings, similar to the zyxin kinetics in hMSCs treated with the ROCK inhibitor, strongly indicate that 350 nm gratings reduces intracellular tension in hMSCs. The comparable magnitude on how Y27632 and the 350 nm gratings affect intracellular tension [6,22] also suggests that this particular topography reduces intracellular tension to a similar extent as a compliant substrate.

5. Conclusion

This study demonstrates that 350 nm grating topography affects hMSC adhesion and migration. Our data identified zyxin as part of the molecular machinery responsible for this response. We show that hMSCs on 350 nm topography display mature focal adhesions of smaller size and exhibit a higher migratory speed. This in turn leads to significantly decreased zyxin protein expression in the cytosolic and membrane fraction in hMSC cultured on 350 nm gratings. Since zyxin's association is driven by force exerted on FA, we propose that 350 nm grating topography decreases intracellular tension. A higher turnover rate of zyxin has been described previously for cells cultured on compliant substrates [22]; therefore we conclude that the initial molecular response to 350 nm topography is similar to that of a cellular response to a compliant substrate.

Acknowledgements

We would like to thank Dr. David Baltimore, Dr. Trono, Dr. Rottner and Dr. Petroll for sharing their plasmids, Dr. Prockop for the hMSCs, Dr. Sam Johnson and Dr. Yasheng Gao for excellent assistance with the confocal microscopes and Allie Speidel and Michelle Gignac for help with the scanning electron microscope. This work was supported by the NIH grant HL83008, and K.K. was supported by the fellowship PA00P3_124163 of the Swiss National Science Foundation.

References

[1] McMurray RJ, Gadegaard N, Tsimbouri PM, Burgess KV, McNamara LE, Tare R, et al. Nanoscale surfaces for the long-term maintenance of mesenchymal stem cell phenotype and multipotency. Nat Mater 2011;10:637–44.
[2] Dalby MJ, Gadegaard N, Tare R, Andar A, Riehle MO, Herzyk P, et al. The control of human mesenchymal cell differentiation using nanoscale symmetry and disorder. Nat Mater 2007;6:997–1003.
[3] Yim EK, Pang SW, Leong KW. Synthetic nanostructures inducing differentiation of human mesenchymal stem cells into neuronal lineage. Exp Cell Res 2007;313:1820–9.
[4] Kulangara K, Leong KW. Substrate topography shapes function. Soft Matter 2009;5:4072–6. Highlight.
[5] Pittenger MF, Mackay AM, Beck SC, Jaiswal RK, Douglas R, Mosca JD, et al. Multilineage potential of adult human mesenchymal stem cells. Science 1999; 284:143–7.
[6] Engler AJ, Sen S, Sweeney HL, Discher DE. Matrix elasticity directs stem cell lineage specification. Cell 2006;126:677–89.
[7] McBeath R, Pirone DM, Nelson CM, Bhadriraju K, Chen CS. Cell shape, cytoskeletal tension, and RhoA regulate stem cell lineage commitment. Dev Cell 2004;6:483–95.
[8] Kilian KA, Bugarija B, Lahn BT, Mrksich M. Geometric cues for directing the differentiation of mesenchymal stem cells. Proc Natl Acad Sci USA 2010;107: 4872–7.
[9] Hynes RO. Integrins: bidirectional, allosteric signaling machines. Cell 2002; 110:673–87.
[10] Martin KH, Slack JK, Boerner SA, Martin CC, Parsons JT. Integrin connections map: to infinity and beyond. Science 2002;296:1652–3.
[11] Kanchanawong P, Shtengel G, Pasapera AM, Ramko EB, Davidson MW, Hess HF, et al. Nanoscale architecture of integrin-based cell adhesions. Nature 2010;468:580–4.
[12] Geiger B, Bershadsky A, Pankov R, Yamada KM. Transmembrane crosstalk between the extracellular matrix–cytoskeleton crosstalk. Nat Rev Mol Cell Biol 2001;2:793–805.
[13] Zaidel-Bar R, Cohen M, Addadi L, Geiger B. Hierarchical assembly of cell-matrix adhesion complexes. Biochem Soc Trans 2004;32:416–20.
[14] Ballestrem C, Hinz B, Imhof BA, Wehrle-Haller B. Marching at the front and dragging behind: differential alphaVbeta3-integrin turnover regulates focal adhesion behavior. J Cell Biol 2001;155:1319–32.
[15] Rottner K, Hall A, Small JV. Interplay between Rac and Rho in the control of substrate contact dynamics. Curr Biol 1999;9:640–8.
[16] Galbraith CG, Yamada KM, Sheetz MP. The relationship between force and focal complex development. J Cell Biol 2002;159:695–705.
[17] Riveline D, Zamir E, Balaban NQ, Schwarz US, Ishizaki T, Narumiya S, et al. Focal contacts as mechanosensors: externally applied local mechanical force induces growth of focal contacts by an mDia1-dependent and ROCK-independent mechanism. J Cell Biol 2001;153:1175–86.
[18] Zamir E, Katz M, Posen Y, Erez N, Yamada KM, Katz BZ, et al. Dynamics and segregation of cell-matrix adhesions in cultured fibroblasts. Nat Cell Biol 2000;2:191–6.
[19] Pankov R, Cukierman E, Katz BZ, Matsumoto K, Lin DC, Lin S, et al. Integrin dynamics and matrix assembly: tensin-dependent translocation of alpha(5) beta(1) integrins promotes early fibronectin fibrillogenesis. J Cell Biol 2000; 148:1075–90.
[20] Zaidel-Bar R, Ballestrem C, Kam Z, Geiger B. Early molecular events in the assembly of matrix adhesions at the leading edge of migrating cells. J Cell Sci 2003;116:4605–13.
[21] Hirata H, Tatsumi H, Sokabe M. Mechanical forces facilitate actin polymerization at focal adhesions in a zyxin-dependent manner. J Cell Sci 2008;121: 2795–804.
[22] Lele TP, Pendse J, Kumar S, Salanga M, Karavitis J, Ingber DE. Mechanical forces alter zyxin unbinding kinetics within focal adhesions of living cells. J Cell Physiol 2006;207:187–94.
[23] Lauffenburger DA, Horwitz AF. Cell migration: a physically integrated molecular process. Cell 1996;84(3):359–69.
[24] Huttenlocher A, Ginsberg MH, Horwitz AF. Modulation of cell migration by integrin-mediated cytoskeletal linkages and ligand-binding affinity. J Cell Biol 1996;134:1551–62.
[25] Yim EK, Reano RM, Pang SW, Yee AF, Chen CS, Leong KW. Nanopattern-induced changes in morphology and motility of smooth muscle cells. Biomaterials 2005;26:5405–13.
[26] Bao LR, Cheng X, Huang XD, Guo LJ, Pang SW, Yee AF. Nanoimprinting over topography and multilayer three-dimensional printing. J Vac Sci Technol B 2002;20:2881–6.
[27] Yim EK, Darling EM, Kulangara K, Guilak F, Leong KW. Nanotopography-induced changes in focal adhesions, cytoskeletal organization, and mechanical properties of human mesenchymal stem cells. Biomaterials 2009;31: 1299–306.
[28] Wolfe M, Pochampally R, Swaney W, Reger RL. Isolation and culture of bone marrow-derived human multipotent stromal cells (hMSCs). Methods Mol Biol 2008;449:3–25.
[29] Reger RL, Wolfe MR. Freezing harvested hMSCs and recovery of hMSCs from frozen vials for subsequent expansion, analysis, and experimentation. Methods Mol Biol 2008;449:109–16.
[30] Reger RL, Tucker AH, Wolfe MR. Differentiation and characterization of human MSCs. Methods Mol Biol 2008;449:93–107.
[31] Lois C, Hong EJ, Pease S, Brown EJ, Baltimore D. Germline transmission and tissue-specific expression of transgenes delivered by lentiviral vectors. Science 2002;295:868–72.
[32] Chalut KJ, Kulangara K, Giacomelli MG, Wax A, Leong KW. Deformation of stem cell nuclei by nanotopographical cues. Soft Matter 2010;6:1675–81.
[33] Rottner K, Krause M, Gimona M, Small JV, Wehland J. Zyxin is not colocalized with vasodilator-stimulated phosphoprotein (VASP) at lamellipodial tips and exhibits different dynamics to vinculin, paxillin, and VASP in focal adhesions. Mol Biol Cell 2001;12:3103–13.
[34] Hirata H, Tatsumi H, Sokabe M. Zyxin emerges as a key player in the mechanotransduction at cell adhesive structures. Commun Integr Biol 2008;1: 192–5.
[35] Kantawong F, Burchmore R, Gadegaard N, Oreffo RO, Dalby MJ. Proteomic analysis of human osteoprogenitor response to disordered nanotopography. J R Soc Interface 2008;6:1075–86.
[36] Peyton SR, Putnam AJ. Extracellular matrix rigidity governs smooth muscle cell motility in a biphasic fashion. J Cell Physiol 2005;204:198–209.
[37] von Wichert G, Haimovich B, Feng GS, Sheetz MP. Force-dependent integrin-cytoskeleton linkage formation requires downregulation of focal complex dynamics by Shp2. EMBO J 2003;22:5023–35.
[38] Chrzanowska-Wodnicka M, Burridge K. Rho-stimulated contractility drives the formation of stress fibers and focal adhesions. J Cell Biol 1996;133: 1403–15.
[39] Balaban NQ, Schwarz US, Riveline D, Goichberg P, Tzur G, Sabanay I, et al. Force and focal adhesion assembly: a close relationship studied using elastic micropatterned substrates. Nat Cell Biol 2001;3(5):466–72.
[40] Pavalko FM, Burridge K. Disruption of the actin cytoskeleton after microinjection of proteolytic fragments of alpha-actinin. J Cell Biol 1991;114:481–91.
[41] Hoffman LM, Jensen CC, Kloeker S, Wang CL, Yoshigi M, Beckerle MC. Genetic ablation of zyxin causes Mena/VASP mislocalization, increased motility, and deficits in actin remodeling. J Cell Biol 2006;172:771–82.